

RESEARCH ARTICLE

Reliability of Response-Controlled Stepped Sine Testing for Experimental Detection of Nonlinear Structure

A. R. Bahari¹, M. A. Yunus^{1,2*}, M. N. Abdul Rani¹, Z. Yahya³ and M. A. Rahim⁴

¹Structural Dynamics Analysis & Validation (SDAV), College of Engineering, Universiti Teknologi MARA (UiTM), 40450 Shah Alam, Selangor, Malaysia

²Institute for Infrastructure Engineering and Sustainable Management (IIESM), Universiti Teknologi MARA (UiTM), 40450 Shah Alam, Selangor, Malaysia

³Kolej Universiti Poly-Tech MARA, 56100, Kuala Lumpur, Malaysia

⁴Faculty of Electrical Engineering Technology, Universiti Malaysia Perlis Pauh Putra Campus, 02600 Arau, Perlis, Malaysia

ABSTRACT - Nonlinear structural dynamic analysis is required for mechanical structures experiencing nonlinearity through large force-vibration response ranges. Nonlinearities can be caused by large vibration displacements, material properties, or joints. Experimental modal analysis for nonlinear detection is achieved using conventional force-controlled stepped sine testing. However, this approach often encounters premature jumps in frequency response curves before reaching actual resonance peaks. In recent years, response-controlled stepped sine testing (RCT) has been introduced to quantify resonant peaks precisely. This approach, however, has only been limitedly utilised to detect and analyse nonlinearity in jointed structures and structures experiencing large displacement. In this paper, the reliability of the RCT approach is assessed for detecting nonlinearity from different sources. The experimental setup involves placing two magnets on opposite sides of a plate's free end to induce localised nonlinearity through magnet attraction. A low force magnitude of random excitation is employed to identify the frequency range of the first vibration mode using an electromagnetic shaker. Subsequently, RCT is performed within this range to measure the nonlinear forced response. Frequency response functions are measured at ten different controlled displacement amplitudes at the driving point. The analysis observed a symmetry curve of response in the measured FRFs. The results indicate that nonlinear hardening is detected at structures with localised magnet attraction. In conclusion, the reliability of applying the RCT approach for detecting nonlinearity from magnet attraction is achieved due to the absence of a jump issue in FRFs.

ARTICLE HISTORY

Received	: 07 th March 2023
Revised	: 19 th July 2023
Accepted	: 22 nd Aug 2023
Published	: 26 th Sept 2023

KEYWORDS

Nonlinear dynamic;
Nonlinear detection;
Response-controlled stepped sine test;
Structural vibration;
Modal analysis

1.0 INTRODUCTION

The nonlinear dynamic characteristic should be considered in the design and analysis of engineering structures [1] to obtain more realistic predictions and to prevent catastrophic collapses when these structures operate in nonlinear zones [2]. This concern becomes particularly significant for aerospace structures, which operate in a nonlinear regime under various designs, extreme loads, and varying environmental conditions. As a result, the effects of nonlinear dynamic characteristics are of primary importance and have attracted the interest of researchers for many years. Numerous nonlinearity effects can occur from a variety of sources, including jointed interfaces in assembled structures [3], [4], variations in material parameters [5], geometric effects [6], boundary conditions, impacts [7] and contact phenomena [8].

In vibration testing, nonlinear experimental modal analysis (EMA) is used to detect and characterise nonlinear properties of structures. Much research has been carried out in the field of nonlinear detection to identify the types and parameters of nonlinearity using vibration test data [9] – [11]. It is well known that the availability of nonlinear dynamic responses of a structure is highly dependent on the type of input dynamic excitation [12]. Investigating the reliability of the various dynamic excitations is crucial for effectively detecting nonlinearity in structures. Moreover, nonlinear structures respond differently in different ways to different types of input excitations. Therefore, it is necessary to evaluate the ability of the different excitation approaches to detect nonlinearity.

In random vibration tests, all frequencies of a defined spectrum are excited simultaneously at a given time of excitation. The total power in the excitation of the input spectrum is distributed over the defined frequency band. The structural resonances can be excited simultaneously due to the numerous forcing frequencies. However, the random excitation may not always be able to sufficiently excite the structural nonlinearity, as averages are used to improve FRF coherence. The amplitude and phase of the random excitation signal often produce undistorted FRFs [11].

To overcome this problem, researchers in the field of structural dynamics use sine sweep testing to detect nonlinearity. The frequency of sinusoidal harmonic excitation changes as a function of time with an equal input power level over a

prescribed frequency range of interest [13]. During the sweep sine run test, the load level depends on the input force and the sweep rate, which can be either linear or logarithmic. This well-established broad-band excitation technique is relatively fast and widely used for measuring FRFs [14]–[16].

In nonlinear EMA, force-controlled stepped sine testing is widely used for nonlinear investigations [17]. Nonlinear detection is achieved by varying the input force to determine the frequency response of structures [14]. However, the limitation of this classical approach is that it does not give satisfactory results for structures with strong nonlinearity. A premature jump in the frequency response curves can be detected before the actual resonant peak is reached. In addition, unstable branches and turning points of nonlinear frequency response curves are often overlooked in constant force and stepped sine testing frequently due to the limitations of the test algorithms available in commercial equipment to measure unstable branches.

In contrast, an alternative approach known as response-controlled stepped sine testing (RCT) is proposed in EMA for nonlinear structures. It is a systematic extension of nonlinear phase resonance testing. In this experimental technique, the amplitude of the displacement response of a structure at the driving point is constantly controlled during stepped sine sinusoidal excitation. The magnitude of harmonic force excitation at the driving point is adjusted. The displacement amplitude is constant at each discrete frequency within the frequency range of the vibration mode. In modal analysis, the equation of motion for the dynamic response of a linear model describing structural motion is a second-order differential equation [18]–[20], as in Eq. (1).

$$[M]\{\ddot{x}\} + [C]\{\dot{x}\} + [K]\{x\} = \{F\} \quad (1)$$

where $[M]$, $[C]$ and $[K]$ are the mass, damping and stiffness matrices. $\{\ddot{x}\}$, $\{\dot{x}\}$ and $\{x\}$ are the $n \times 1$ acceleration, velocity and displacement vectors, respectively. $\{F\}$ is an external excitation force vector in harmonic characteristic as in Eq. (2).

$$\{F\} = f \sin(\omega t) \quad (2)$$

where f is force magnitude, ω is frequency, and t is time. For a nonlinear structure, the equation of motion [10] consists of nonlinear parameters, as shown in Eq. (3).

$$[M]\{\ddot{x}\} + [C]\{\dot{x}\} + [K]\{x\} + [F_{NL}]\{x, \dot{x}\} = \{F\} \quad (3)$$

where F_{NL} is a nonlinear force in a function of displacement and velocity. Equation of motion of a nonlinear structure subjected to a harmonic excitation ω in the form of frequency domain as in Eq. (4) where $\{X\}$ is the vector of displacement.

$$-\omega^2[M]\{X\} + i\omega[C]\{X\} + [K]\{X\} + [F_{NL}]\{X\} = \{F\} \quad (4)$$

The nonlinear eigenvalue problem is associated with the conservative part, as in Eq. (5).

$$([K] + [F_{NL}]_{re})\{\bar{\varphi}\}_r = \bar{\omega}_r^2 [M]\{\bar{\varphi}\}_r \quad (5)$$

where $\{\bar{\varphi}\}_r$ is the r^{th} real-valued nonlinear normal mode and $\bar{\omega}_r$ is the natural frequency. The vectors of displacement amplitude can be calculated using Eq. (6), where $\{\bar{\vartheta}\}_r$ is calculated as in Eq. (7).

$$\{X\} = \frac{\{\bar{\vartheta}\}_r \{\bar{\vartheta}\}_r^T \{F\}}{\bar{\omega}_r^2 - \omega^2 + i\tau_r \bar{\omega}_r^2} \quad (6)$$

$$\{\bar{\vartheta}\}_r = \frac{\{\bar{\varphi}\}_r}{\sqrt{m_r}} \quad (7)$$

The near-resonant receptance $\bar{\alpha}_{jk}$ at point j for a given excitation at point k can be calculated as in Eq. (8).

$$\bar{\alpha}_{jk} = \frac{\bar{\vartheta}_{jr} \bar{\vartheta}_{kr}}{\bar{\omega}_r^2 - \omega^2 + i\bar{\eta}_r \bar{\omega}_r^2} \quad (8)$$

where $\bar{\eta}_r$ is nonlinear hysteretic modal damping. Using RCT, the near-resonant receptance $\bar{\alpha}_{jk}$ can be determined as in Eq. (9) where \bar{A}_{jkr} is a complex valued modal constant.

$$\bar{\alpha}_{jk} = \frac{\bar{A}_{jkr}}{\bar{\omega}_r^2 - \omega^2 + i\bar{\eta}_r \bar{\omega}_r^2} \quad (9)$$

The measured constant-response FRFs are in quasi-linearised form due to the constant modal amplitude during the RCT strategy [22]. Therefore, the modal parameters in the mode of interest are extracted as a function of modal amplitude by applying standard linear modal analysis techniques. Several researches have used this approach to experimentally detect nonlinearities from various nonlinear sources. Using this approach, [21] discovered the geometrical nonlinearity of a double-clamped thin beam structure due to large amplitude oscillations. [22] used the RCT method to find damping nonlinearity caused by microslip in the beam-base connections.

This article focuses on evaluating the reliability of applying RCT to detect structural nonlinearity, with specific attention to a structure featuring magnet attraction. Initially, linear EMA is conducted to determine the linear natural frequency of the first mode. Subsequently, nonlinear EMA is performed to measure the linear dynamic response of the structure. The measured FRFs are analysed to gain insight into the frequency response curves and resonant frequencies. Through a detailed analysis of the FRF characteristics, the reliability of the RCT approach in detecting nonlinearity in structures with magnet attraction is thoroughly assessed.

2.0 TEST SETUP AND PROCEDURES

A thin steel plate 190.0 mm long with a rectangular cross-section 25.0 mm wide and 1.0 mm thick was used in the nonlinear investigation. Figure 1 shows the experimental setup for linear and nonlinear modal analysis. The plate was held vertically with fixed-free conditions. One end of the plate was fixed in y-direction and z-direction by a rigid and stiff clamp. The other end of the plate was free in the x-direction for bending modes.



Figure 1. Experimental setup for linear and nonlinear modal analysis

A schematic diagram for the EMA is illustrated in Figure 2. Two magnets were symmetrically positioned on either side of the plate tip. The magnetic attraction was introduced at the free end of the plate tip. A careful and precise setup ensured that there was a consistent distance of 60.0 mm between the two magnets in the equilibrium position, with equal distances of 30.0 mm on each side of the plate.

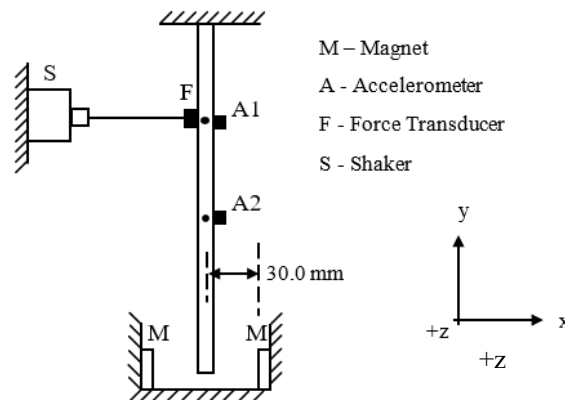


Figure 2. Magnets located at the plate tip

EMA was performed with a dynamic excitation source consisting of an electromagnetic shaker powered by an amplifier. The shaker was fixed to a rigid steel module. This permanent shaker was placed near the clamp. A force transducer was attached to the plate with strong adhesive to measure the excitation force exerted by the shaker via a stinger. It is worth noting that the position of the excitation point near the fixed clamp was chosen to minimise the interaction at large vibration amplitudes. The interaction between the shaker and the plate was carefully adjusted to minimise external bias and misalignment. Two accelerometers were used to measure the fundamental frequency. Accelerometer 1 was located at the driving point and served as a reference channel for control purposes. Accelerometer 2 was positioned 30.0 mm below the driving point to measure the vibration response where the fundamental mode shape has a large deflection. Accelerometer 2 was not placed at the plate tip to ensure accurate measurements while avoiding any interference with the magnet attraction.

The EMA was carried out according to the steps in the schematic flow chart in Figure 3. In the first work, random excitation testing was performed to obtain the linear frequency response function of the plate. The result was a fundamental frequency for the first mode in large deflection in the x-axis. The EMA continued with nonlinear dynamic

testing. The frequency range of the first mode was decided based on the linear dynamic testing results. In the RCT technique, several displacement amplitudes were chosen as the control parameter. A comparison between all the measured FRFs was conducted to identify the nonlinearity due to magnetic attraction.

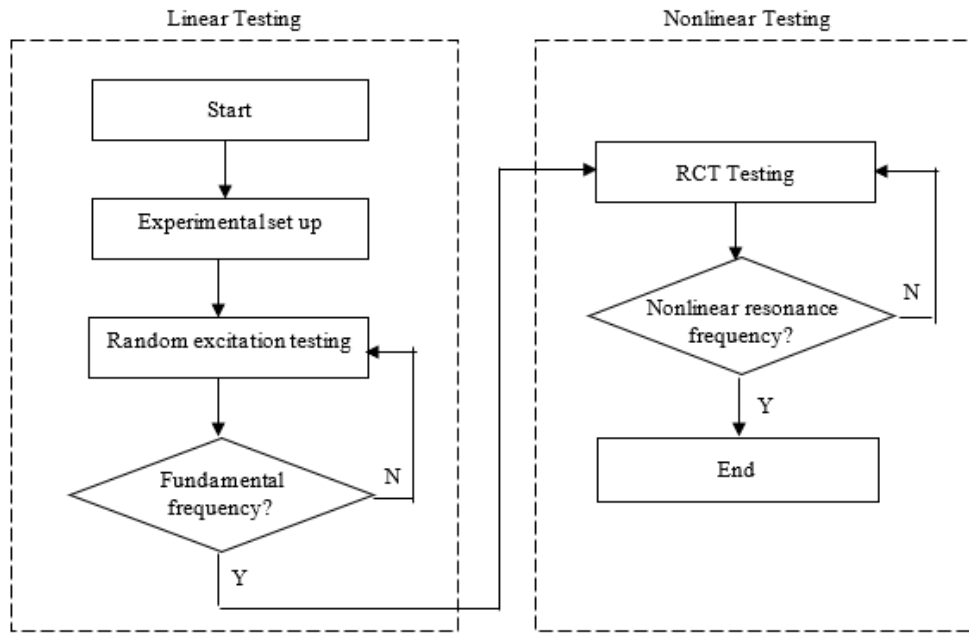
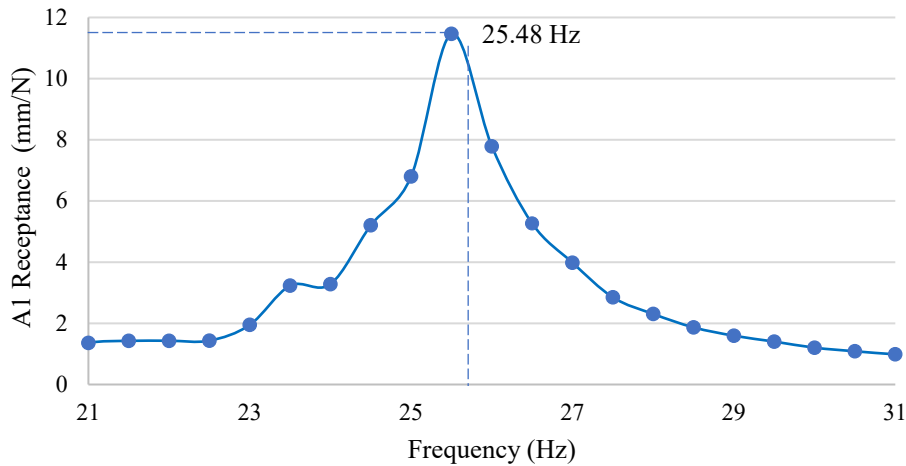


Figure 3. Flow chart of proposed assessment for RCT reliability

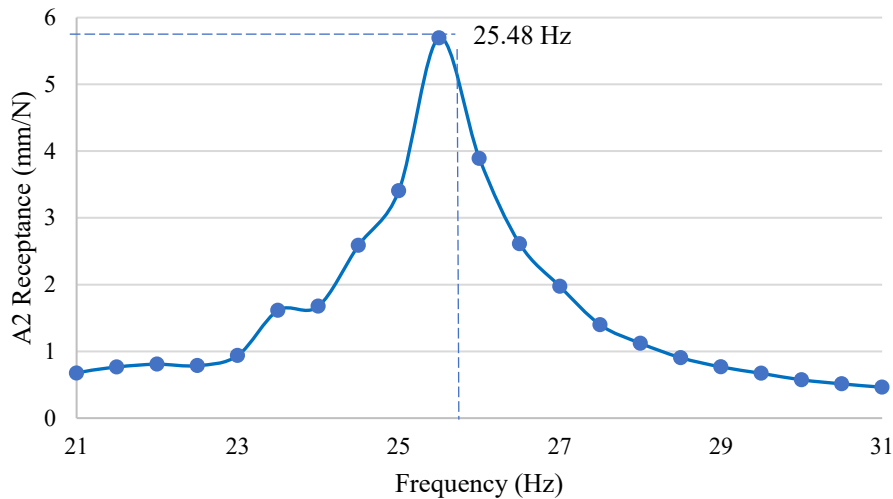
3.0 LINEAR EXPERIMENTAL MODAL ANALYSIS

The investigation started with a conventional experimental modal analysis (EMA) to determine the first mode of the plate. In this work, only the fundamental linear dynamic characteristic is considered in the analysis. A burst random of white noise characteristic was used for the input excitation. This test is known as a linear EMA due to the low force magnitude of excitation. The FRFs were measured and analysed to identify the linear dynamic characteristic. The linear natural frequency and modal damping ratios were estimated using the LMS Test.Lab Polymax identification algorithm. Figure 4 shows the receptance FRFs measured at points 1 and 2.



(a)

Figure 4. Measured FRFs using burst random excitation (a) point 1



(b)

Figure 4. (cont.) Measured FRFs using burst random excitation (b) point 2

The frequency range of the first mode, as determined from the linear EMA, ranges between 21.0 Hz and 31.0 Hz. Further details about the resonant frequency can be found in Table 1, which specifically lists the resonant frequency as 25.48 Hz. It is worth noting that the FRFs exhibited an identical shape for both points 1 and 2. However, the amplitude of the FRF at point 1 exceeds that of point 2. Specifically, the amplitude at point 1 was 11.46 mm/N, significantly higher than the amplitude at point 2, which measured 5.69 mm/N. This difference is due to the application of the excitation force at driving point 1.

Table 1. Natural frequency measured from linear EMA

Point	Accelerometer	Natural frequency (Hz)	Receptance amplitude (mm/N)
1	A1	25.48	11.46
2	A2	25.48	5.69

4.0 RESPONSE-CONTROLLED STEPPED SINE TESTING

The nonlinear element was introduced into the structure by placing two magnets on both sides of the plate's free end. Ten different controlled-displacement amplitudes were employed at the driving point (point 1) to conduct the nonlinear EMA. Following the RCT approach, point 1 was initially excited at a discrete frequency of 21.0 Hz, and its displacement amplitude was set to 0.50 mm. The harmonic force magnitude at point 1 was adjusted by a shaker in order to achieve the desired 0.50 mm displacement amplitude. The excitation frequency began at 21.0 Hz and gradually increased with a step of 0.125 Hz, covering the frequency range of the first mode (from 21.0 Hz to 31.0 Hz). A closed loop control mechanism was utilised to maintain a constant displacement amplitude at point 1 throughout the measurements. The entire process was repeated for ten different controlled-displacement amplitudes, providing comprehensive data for analysis and comparison.

The steady-state vibration response was carefully measured at each frequency step, and the resulting data was directly compared in both frequencies and phases. Figure 5 shows the measured nonlinear FRFs for points 1 and 2. The controlled displacement was initially set to 0.50 mm and then increased in steps of 0.20 mm, reaching a maximum displacement amplitude of 2.20 mm. From the figures, it is shown that controlled displacement has a significant impact on the resonant frequency, particularly in the first mode. The distortion was apparent in the FRFs at high controlled displacement, creating a clear difference from the FRFs measured at lower controlled displacement amplitudes. Specifically, at a controlled displacement of 0.5 mm, the plate's response exhibits characteristics similar to a linear dynamic response. However, as the controlled displacement amplitude increases, the presence of the magnets causes an obvious nonlinearity effect, which directly affects the resonant frequency.

The resonant frequency demonstrates an increase as the controlled displacement amplitude is increased. The shifting of the FRFs towards higher frequencies indicates a significant hardening of nonlinear behaviour. Notably, a symmetrical shifting of the resonance frequency towards a higher frequency was observed, and no jump phenomenon was detected in the measured FRFs prior to reaching the actual resonance peak. Additionally, the increase in controlled displacement directly leads to an increase in the FRF amplitude, indicating a decrease in damping. Consistent results were obtained for point 2.

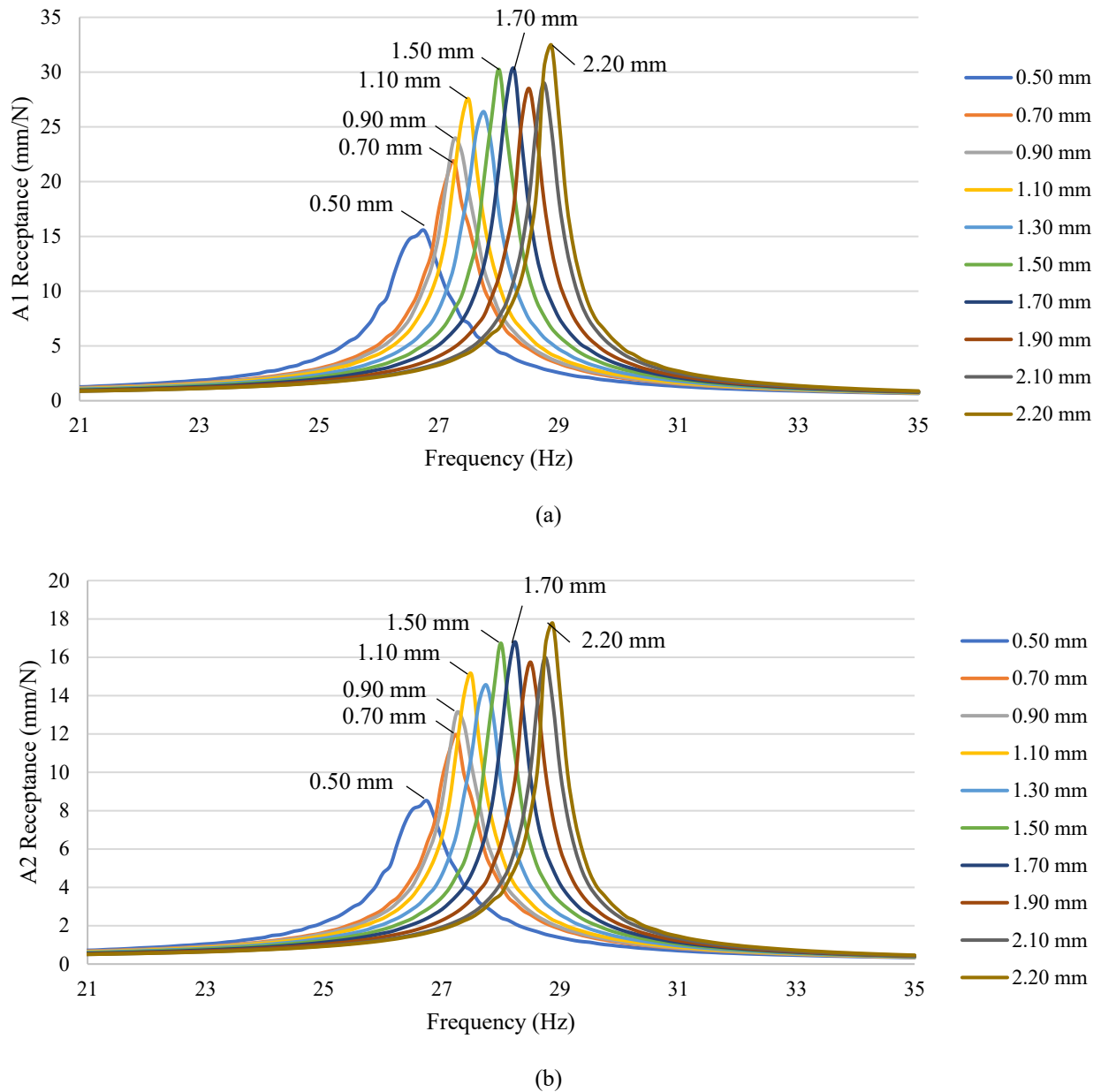


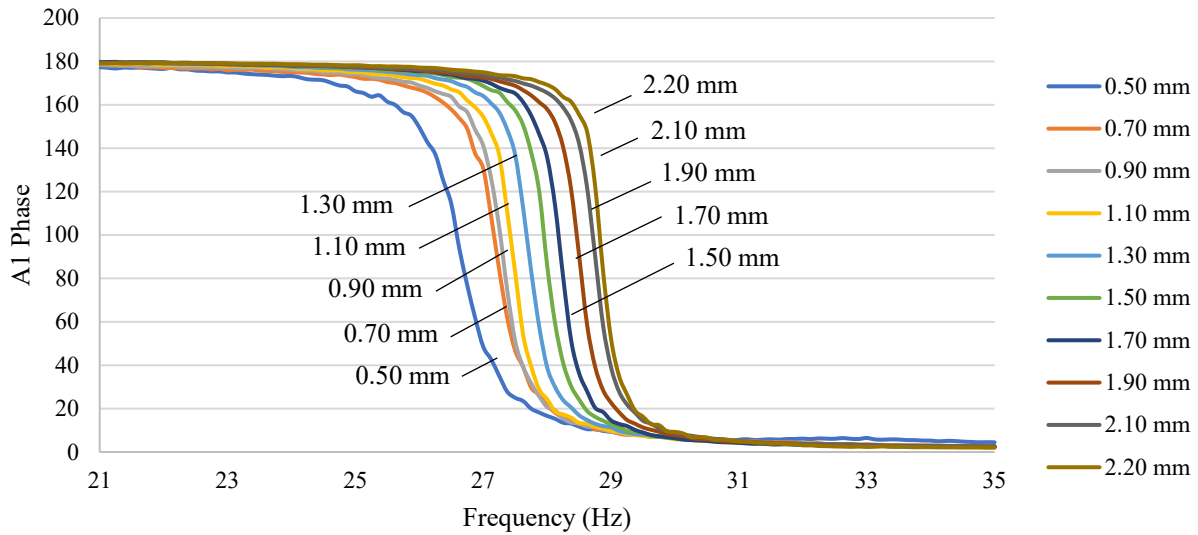
Figure 5. Measured frequency response function (a) point 1 (b) point 2

The FRF peaks were extracted to determine the resonant frequencies precisely. Table 2 lists the resonant frequencies corresponding to ten controlled displacement amplitudes. Clearly, at a controlled displacement of 0.5 mm, the resonant frequency measured 26.75 Hz, slightly exceeding the linear resonant frequency obtained from the linear EMA. The resonant frequency increases with the increase in controlled displacement, indicating a hardening nonlinearity due to the magnetic attraction. Furthermore, with each increase in controlled displacement, the resonant frequency exhibited an increasing pattern. At a displacement of 2.2 mm, the resonant frequency reached 28.87 Hz, showing the increasing impact of the magnetic attraction-induced hardening nonlinearity.

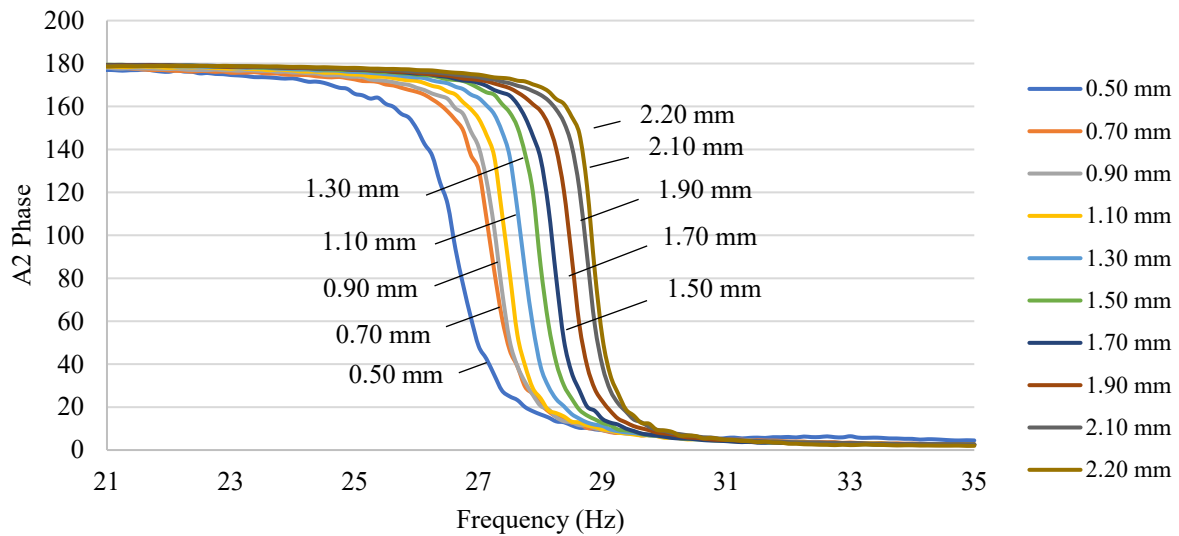
Table 2. Resonant frequency of controlled displacement during the RCT

Run	Controlled displacement (mm)	Frequency (Hz)
1	0.5	26.75
2	0.7	27.25
3	0.9	27.25
4	1.1	27.50
5	1.3	27.75
6	1.5	28.00
7	1.7	28.25
8	1.9	28.50
9	2.1	28.75
10	2.2	28.87

Figure 6 presents a comprehensive comparison of the phase spectrums at incremental values of controlled displacement, ranging from 0.50 mm to 2.20 mm, for points 1 and 2. Clearly, the results show a consistent shift towards higher frequencies in the measured phase spectrum as the controlled displacement increases. In summary, the assessment conclusively demonstrates the reliability of RCT in experimentally detecting nonlinearity throughout the entire frequency range, attributed to the magnetic attraction source. The dynamic response, particularly in the resonant region, is strongly influenced by the magnetic attraction phenomenon. This is evident through the observation of a distinct hardening effect, with the resonant frequency shifting approximately 8% for a 2.20 mm controlled-displacement amplitude exhibiting symmetrical characteristics.



(a)



(b)

Figure 6. Measured phase spectrum (a) point 1 (b) point 2

5.0 CONCLUSIONS

The reliability of a recent approach in nonlinear experimental modal analysis (EMA) called response-controlled stepped sine testing (RCT) for detecting localised nonlinearity resulting from magnet attraction is discussed in this paper. The investigation started with linear dynamic analysis, employing random excitation with a white noise characteristic. The linear dynamic response of a fixed-free plate subjected to a magnet attraction field was measured using a low excitation force magnitude to determine the frequency range of the first mode. For nonlinear EMA, RCT was performed with ten different controlled displacement amplitudes at the driving point. The harmonic force magnitude was adjusted to maintain the displacement amplitude. There was no presence of jump phenomena in the results, as from the symmetry of the FRFs. The resonant frequencies shifted, and the FRFs' amplitude increased proportionally with the controlled displacement amplitudes, indicating some form of hardening in the nonlinearity. Overall, the RCT approach proved highly

reliable in accurately detecting nonlinearity within a nonlinear system characterised by localised nonlinearity arising from magnet attraction.

6.0 ACKNOWLEDGEMENT

The authors wish to acknowledge the Kolej Universiti Poly-Tech MARA (KUPTM) and Research Management Centre (RMC) for providing financial support for this research through the research grant scheme KUPTM.DVCRI.RMC.15 (41). The authors would also like to extend their sincere gratitude to Structural Dynamics Analysis & Validation (SDAV) of UiTM for the support and facilities.

7.0 REFERENCES

- [1] W. Sun, T. Li, D. Yang, Q. Sun, and J. Huo, "Dynamic investigation of aeroengine high pressure rotor system considering assembly characteristics of bolted joints," *Engineering Failure Analysis*, vol. 112, p. 104510, 2020.
- [2] D. J. Ewins, B. Weekes, and A. delli Carri, "Modal testing for model validation of structures with discrete nonlinearities," *Philosophical Transactions of the Royal Society A: Mathematical, Physical and Engineering Sciences*, vol. 373, no. 2051, 2015.
- [3] M. Jin, M. R. W. Brake, and H. Song, "Comparison of nonlinear system identification methods for free decay measurements with application to jointed structures," *Journal of Sound and Vibration*, vol. 453, pp. 268–293, 2019.
- [4] K. Lingfei, J. Heling, A. H. Ghasemi, and L. Yan, "Condensation modeling of the bolted joint structure with the effect of nonlinear dynamics," *Journal of Sound and Vibration*, vol. 442, pp. 657–676, 2019.
- [5] M. Piraccini and R. Di Sante, "Measurement of nonlinear vibration response in aerospace composite blades using pulsed airflow excitation," *Measurement*, vol. 130, pp. 422–434, 2018.
- [6] A. R. Bahari, M. A. Yunus, M. N. Abdul Rani, M. A. Ayub, and A. Nalisa, "Numerical and experimental investigations of nonlinearity behaviour in a slender cantilever beam," in *MATEC Web of Conferences*, 2018, vol. 217, p. 02008.
- [7] C. A. Herrera, D. M. McFarland, A. L. Bergman, and A. F. Vakakis, "Methodology for nonlinear quantification of a flexible beam with a local, strong nonlinearity," *Journal of Sound and Vibration*, vol. 388, pp. 298–314, 2017.
- [8] M. R. T. Bidhendi, "Nonlinear dynamics of a cantilevered beam with a tip mass and elastic-damping support," *International Journal of Nonlinear Mechanics*, vol. 125, p. 103541, 2020.
- [9] J. Taghipour, H. H. Khodaparast, H. Madinei, and H. Jalali, "Detection of localised nonlinearity in dynamical systems using base excitation experimental results," *Journal of Theoretical and Applied Vibration and Acoustics*, vol. 6, no. 1, pp. 35–50, 2020.
- [10] J. P. Noël, L. Renson, and G. Kerschen, "Complex dynamics of a nonlinear aerospace structure: Experimental identification and modal interactions," *Journal of Sound and Vibration*, vol. 333, no. 12, pp. 2588–2607, 2014.
- [11] K. Worden and G. R. Tomlinson, *Nonlinearity in Structural Dynamics: Detection, Identification and Modelling*. Bristol and Philadelphia: Institute of Physics, 2001.
- [12] D. M. Lobo, T. G. Ritto, D. A. Castello, and E. Cataldo, "Dynamics of a Duffing oscillator with the stiffness modeled as a stochastic process," *International Journal of Nonlinear Mechanics*, vol. 116, pp. 273–280, 2019.
- [13] N. Roy, M. Violin, and E. Cavro, "Sine sweep effect on specimen modal parameters characterisation," *Advances in Aircraft and Spacecraft Science*, vol. 5, no. 2, pp. 187–204, 2018.
- [14] C. Ligeikis, A. Bouma, J. Shim, S. Manzato, R. J. Kuether, and D. R. Roettgen, "Modeling and experimental validation of a pylon subassembly mockup with multiple nonlinearities," *Nonlinear Structures & Systems*, vol. 1, pp. 59–74, 2019.
- [15] A. R. Bahari, M. A. Yunus, M. N. Abdul Rani, A. Nalisa, and M. A. S. A. Shah, "Investigation on the effects of suspension stiffness using experimental modal analysis and finite element model updating," in *IOP Conference Series: Materials Science and Engineering*, 2019, vol. 506, no. 1.
- [16] Y. Lei, S. Luo, and M. He, "Identification of model-free structural nonlinear restoring forces using partial measurements of structural responses," *Advances in Structural Engineering*, vol. 20, no. 1, pp. 69–80, 2017.
- [17] R. M. Lacayo and M. S. Allen, "Updating structural models containing nonlinear Iwan joints using quasi-static modal analysis," *Mechanical Systems and Signal Processing*, vol. 118, pp. 133–157, 2019.
- [18] M. A. Yunus, H. Ouyang, M. N. Abdul Rani, and A. A. M. Isa, "Modal test and model updating for a welded structure made from thin steel sheets," in *20th International Congress on Sound and Vibration*, 2013, pp. 1161–1167.
- [19] M. N. Abdul Rani, H. Ouyang, M. A. Yunus, and B. A. Aminudin, "Model updating for a thin steel sheet welded structure," in *20th International Congress on Sound & Vibration*, 2013, vol. 2, pp. 1138–1145.
- [20] M. A. Yunus, M. N. Abdul Rani, M. S. M. Sani, and M. A. S. Aziz Shah, "Finite element model updating of riveted joints of simplified model aircraft structure," *AIP Conference Proceedings*, vol. 1952, no. 1, p. 020013, 2018.
- [21] T. Karaağaçlı and H. N. Özgüven, "Experimental identification of backbone curves of strongly nonlinear systems by using Response-Controlled Stepped-Sine Testing (RCT)," *Vibration*, vol. 3, no. 3, pp. 266–280, 2020.
- [22] T. Karaağaçlı and H. N. Özgüven, "Experimental modal analysis of nonlinear systems by using response-controlled stepped-sine testing," *Mechanical Systems and Signal Processing*, vol. 146, p. 107023, 2021.